15th Canadian Masonry Symposium
Ottawa, Canada
June 2-5, 2025

Shake table tests on the out-of-plane two-way response of a U-shape masonry structure

Dario Vecchio[i], Babar Ilyas[ii], Nuno Mendes[iii], and Paulo B. Lourenço[iv]

ABSTRACT

Unreinforced masonry (URM) structures are vulnerable to strong earthquakes, due to their limited resistance to dynamic actions. These vulnerabilities often lead to failure or collapse, with out-of-plane mechanisms posing a major threat for existing structures not possessing integral (or box-like) behaviour. Despite the number of uncertainties within structural components, the response is usually governed by macro-elements, such as the main façade and orthogonal walls. Based on the degree of connection, URM structures may experience two types of out-of-plane mechanisms, namely one-way and two-way bending. The former involves a macro-element connected only at its top and bottom, leading to a vertical bending axis. In contrast, the latter occurs with two axes of bending, vertical and horizontal, given the additional connection with the orthogonal walls. Moreover, if the façade is insufficiently restrained at the top and lacks adequate connections with the return walls, overturning of the façade and cracking in the orthogonal walls may occur. Such a complex scenario challenges the understanding of the typical two-way bending behavior of URM structures. Predicting the total capacity of these mechanisms is challenging, and currently, the literature lacks adequate analytical and numerical models. This paper presents an extensive shake-table campaign conducted at the University of Minho to evaluate the two-way bending behaviour of URM structures. A specimen was constructed in a U-shape configuration consisting of a façade and two return walls, made of dry-stack granite blocks, to simulate the behaviour of historical URM structures, and to allow for testing repeatability at large displacements near collapse. The response of the specimen, with fixed geometry and boundary conditions, was observed under different recorded ground motions. The changes in the targeted hybrid mechanisms were observed and conclusions were drawn. Data collected is essential to update existing analytical formulations and to calibrate refined numerical models.

KEYWORDS

Shake table testing, U-shape, Out-of-plane, Overturning, Two-way, Collapse.

[i] Ph.D. Student, University of Minho, ISISE, ARISE, Department of Civil Engineering, Guimarães, , dariovecchio4@yahoo.it
[ii] Ph.D. Student, University of Minho, ISISE, ARISE, Department of Civil Engineering, Guimarães, Portugal, babarilyas7@gmail.com
[iii] Researcher, University of Minho, ISISE, Department of Civil Engineering, Guimarães, Portugal, nunomendes@civil.uminho.com
[iv] Full Professor, University of Minho, ISISE, Guimarães, Portugal, pbl@civil.uminho.pt

INTRODUCTION

The attention towards resilient infrastructures and buildings has increased in recent years, following several catastrophic scenarios caused by natural hazards. Often linked with climate change, recent events have shown unexpected behaviours, and the structures' exposure could shortly worsen. Due to the sudden release of energy, natural hazards, such as earthquakes, can be unpredictable, and vulnerable structures, such as unreinforced masonry (URM), can be subjected to these actions. For example, the recorded time histories (TH) from the February 6, 2023, Kahramanmaraş Earthquake in Turkey and Syria in specific stations have revealed higher Peak Ground Acceleration (PGA) when compared to the spectral accelerations demand imposed by the Turkish Building Code [1] within the 475-year return period [2]. Generally, out-of-plane (OOP) mechanisms are typical responses of URM structures when subjected to horizontal dynamic actions, because of the limited tensile strength of the material constituents (bricks and mortar) and mortar bed joints. In-plane (IP) mechanisms are also generated because of horizontal dynamic actions, however, given the relatively higher strength of the masonry in this direction, they may induce damage such as diagonal-shear cracking and shear-sliding on the mortar beds, rather than failures. Past in-situ observations after the strike of strong ground motions, for example, as reported in [3], [4] have revealed that the most observed failures of residential and monumental URM buildings are due to OOP mechanisms in case of existing structures, in which a box-type behaviour is absent. Due to the unknown degree of connection between structural elements, OOP mechanisms are associated with the collapse of a portion or an element of the structure, as well as overturning [5]. In the past, the analysis of this failure was based on the idealization of the ground accelerations in quasi-static forces applied at the centre of gravity of the structural elements [5], [6]. Many applications are based on such idealisation, including preservation and strengthening techniques for built heritage. Recently, research has revealed the limitations of the quasi-static models, opening the road for other approaches that investigate the capacity to withstand large displacements without reaching the collapse [7], [8]. For example, rocking models are based on solving the equation of motion to predict the response of single blocks (or walls) during dynamic events and consider energy dissipation via impacts, as described in Housner's benchmark study [9]. The reliability of the available rocking models still requires investigation because they lack accuracy when compared with laboratory tests or in-situ observations. As a result, experimental research is needed to expand the available database and address gaps in model calibrations. Due to the complexity of simulating the response, the most robust way to investigate the dynamic OOP response of URM is using shake table testing. Shake tables accurately reproduce any recorded or artificial signals if the action is adequately transferred to the specimen. Within this frame, the present paper discusses the first phase of a large testing program involving a U-Shape specimen made of dry-stack granite blocks. The tests described are part of the Work Package II of the STAND4HERITAGE (S4H) project, which aims at proposing new standards and guidelines for the safeguarding of historic and modern masonry buildings, through extensive analytical and experimental investigation.

TWO-WAY RESPONSE OF DRY-STACK MASONRY

URM structures are vulnerable under dynamic horizontal actions due to the lack of sufficient tensile strength of the constituent materials and at the bond interfaces. Nevertheless, the mortar joints have limited capacity to withstand seismic actions and, together with boundary conditions, can influence the occurrence of OOP mechanisms. Depending on the degree of connections between the structural elements, OOP mechanisms can be divided into one-way and two-way bending. One-way mechanisms usually occur when a slender wall has insufficient lateral connections, leading to the formation of three horizontal hinges, at the top, along the height, and at the bottom connection. Differently, when considering a 3D case including a façade and the lateral walls, two-way bending mechanisms are more likely to occur, because of the formation of horizontal and vertical hinges (along the façade-return wall connections). Such a scenario becomes more complex when considering dry-stack URM structures. Despite most URM buildings being featured with mortar, dry-stack assemblies are a common configuration for both historical and modern structures. As an example, Fig. 1 a) shows a modern residential building on Pico Island belonging to the Acores archipelago, (Portugal), while Fig. 1 b) a building in the Inca citadel (UNESCO World Heritage) of Machu Picchu (Peru). Moreover, the present research focused on the probabilistic seismic response, which require dozens of repetitions. Dry-stack masonry is the only feasible approach in this case and has been experimentally investigated by many researchers in the past [10], [11], [12].

(a) (b)

Fig. 1: Dry-stack masonry examples in the world: (a) residential in Pico Island (Portugal) and historical typology in Machu Picchu (Peru)

Dry-stack means mortar-less and the interaction between blocks is governed by the mechanical properties at the interfaces. Hence, typical two-way OOP mechanisms described in the literature [6] could be highly influenced by the in-plane (IP) resistance of the return walls. In the study proposed by [13], these responses are called hybrid mechanisms. A hybrid mechanism is the superposition of an OOP mechanism occurring at the façade together with a diagonal-shear cracking in the return walls. As an example, Fig. 2 shows the idealized hybrid mechanism.

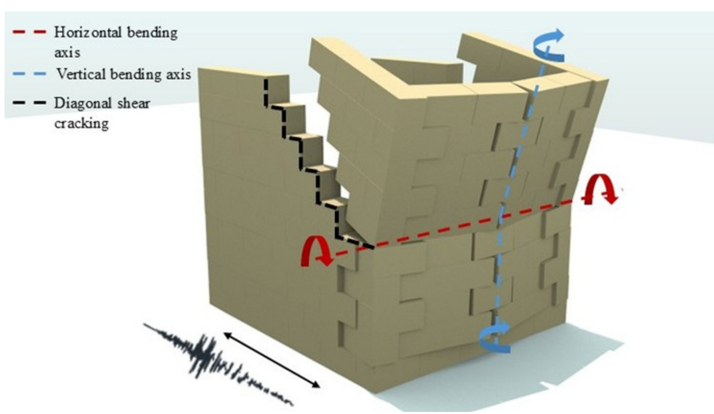

Fig. 2: Theoretical two-way hybrid mechanism showing vertical bending (blue), overturning (red) of the façade, and shear-diagonal cracking (black) in the return walls

While previous experimental studies have investigated the two-way bending response of mortared structures [14], [15], [16], the current knowledge of dry-stack URM structures is scarce. The following Sections describe the details of the present campaign, including the description of the test setup, the choice and the pre-processing of the selected signals, the acquisition system, the validation procedure, the test results, and the conclusions.

THE EXPERIMENTAL CAMPAIGN

Setup

The used 1D shake table facility is located at the Structures Laboratory of the University of Minho, Portugal. The shake table platform is equipped with an accelerometer and a Linear Variable Displacement Transducer (LVDT) The hydraulic actuator has a maximum capacity of 300 kN and can apply accelerations up to 5 g and velocities up to 85 cm/s if the specimen does not exceed total weight of 3 tonnes. In addition, the maximum stroke is ±12.5 cm. A view of the shake table installed at the University of Minho is shown in Fig. 3.

Fig. 3: 1D shake table of the University of Minho

To investigate the occurrence of hybrid mechanisms, numerous tests were conducted on a U-Shape dry-stack half-scale specimens with no diaphragm/roof system, following the assumption of insufficient top connection and lack of adequate state of precompression. The single-leaf specimen consisted of a main façade and two return walls, with running courses. The walls had a constant height of 1.8 m, a façade length of 1.2 m and return walls length of 1.65m, for a total mass of 2.1 tonnes. The masonry consisted of granite blocks of 0.3 m x 0.15 m x 0.15 m and 0.15 m x 0.15 m x 0.15 m dimensions, which were made available from a local company, and provided with a CNC high- precision cutting technique. The mechanical characteristics of the granite blocks are reported in Table 1 [17], where k_n and k_s are the stiffness in the normal and tangential directions, respectively.

Table 1: Mechanical properties of the blocks and interface stiffness

Density (kg/m^3)	E (GPa)	f_c (MPa)	k_n (MPa/mm)	k_s (MPa/mm)
2700	71	140	10	0.4

The constraints imposed by the hydraulic actuator's limitations required a light design in terms of the final setup weight. For this reason, no additional steel frame was brought on top of the shake table. The connection between the specimen and the shake table platform was provided by drilling each bottom block with a pair of M18 bolts. These bolts passed through a drilled 20 mm S275 steel plate aligned with the M27 holes of the shake table platform. Also, the ends of the return walls were constrained against IP deformations by installing two systems composed of two extension springs, two threaded rods, and a hollow beam. The extension springs were available from a previous shake table campaign and fitted the purpose of not adding any further load on the platform. Also, they are adequate to trigger the desired failure mechanism, which has been regularly observed in case of earthquakes affecting old masonry buildings. Fig. 4 shows two views of the U-shape, including the steel plate (in blue) and the extension springs at the end of each return wall. No diaphragms or roof were added, because existing masonry buildings usually lack horizontal elements well connected to the masonry perimetral walls.

a) b)

Fig. 4: Views of the final U-shape specimen: a) main façade and east return wall, b) west return wall

Dynamic identification tests

Dynamic identification tests were carried out to evaluate the effectiveness of the boundary conditions and to identify the modes of the specimen. Despite the high challenges related to the identification of modal properties of dry-stack structures, two setups were planned, one with and one without the application of the extension springs. For each test, 15 accelerometers (ACC, ±0.5 g) were glued on specific blocks of the structure. The specimen was excited with a low-amplitude white noise with a frequency range of 0-50 Hz. Fig. 5 shows the location of the accelerometers on each wall for both tests.

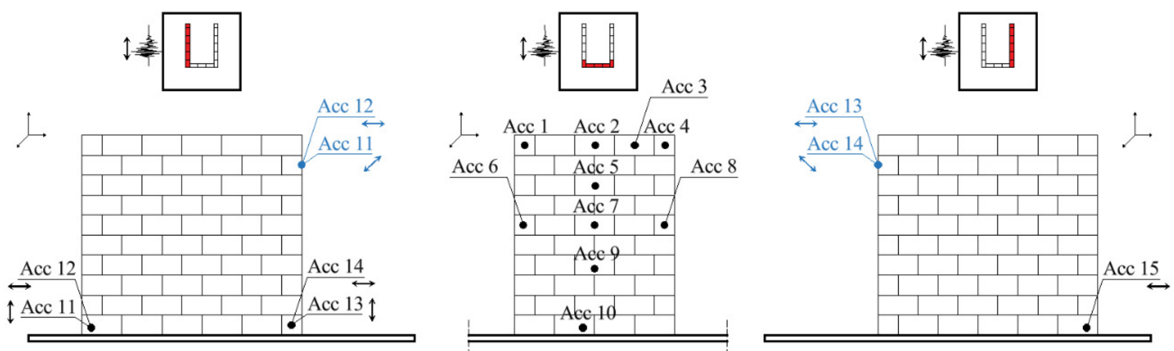

Fig. 5: Location of the accelerometers used for the dynamic identification tests. In black the setup used for the first test (with extension springs) and in blue the changes adopted for the second test (without extension springs)

Because the excitation was known, the frequencies were picked in the commercial software ARTeMIS following the Experimental Modal Analysis (EMA) approach,. As theoretically expected, both tests showed similar responses, with a first modal shape indicating horizontal bending of the facade. Two natural frequencies were identified, associated with increasing curvature points of the horizontal bending profile. Fig. 6 reports the extracted natural frequencies and the respective mode shapes.

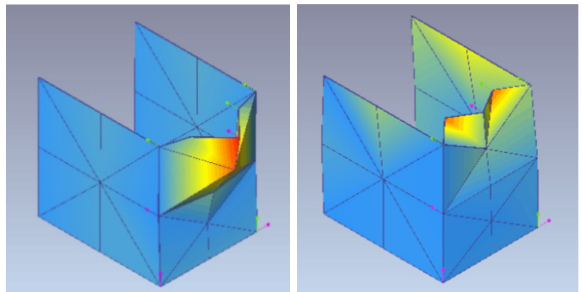

f_1 = 15.38 Hz f_2 = 16.84 Hz

Fig. 6: Dynamic identification tests: natural frequencies and mode shapes

Choice and pre-processing of the selected signals

According to previous theoretical [7] and experimental studies [18], [19], rocking is triggered by the PGA content, while the collapse (overturning) is dictated by the PGV content. Several recorded ground motions were selected from the ESM database according to their acceleration and velocity content and considering the limitations of the shake table when scaling up the records. The responses due to each ground motion were observed in preliminary Non-Linear Time History Analyses (NLTHAs) on a discontinuous model of the U-shape built in the commercial software Abaqus. According to the results of the numerical analyses, the event PT-1998-0019 was chosen because it showed the occurrence of the targeted hybrid mechanism (Fig. 2). Further, a second event, EMSC-2016-0130, was selected to investigate any changes in the targeted mechanism because of its different characteristics. Following [20], the PT-1998-0019 event is a moderate pulse-like signal, while the EMSC-2016-0130 event is a non-pulse-like signal. Due to the shake table stroke limitation, the EMSC-2016-0130 signal required filtering. A Butterworth filter, with cut-off frequencies of 0.2 and 6 Hz, N=4 poles, was applied to eliminate the low-frequency content in the displacement time history and the high-frequency content in the acceleration time history. Additionally, this signal was cut along its time length, to reduce the computation time required by the Digital Image Correlation (DIC) of the shake table and the size of the recorded data. While **Error! Reference source not found.** reports the final summary of the selected signals, Fig. 7 shows the acceleration, velocity, and displacement time histories of the selected signals.

Table 2: Main seismic parameters of the signals selected for the testing program

Event name	PGA (g)	PGV (cm/s)	PGD (cm)
PT-1998-0019	0.37	34.76	3.74
EMSC-2016-0130	0.76	28.92	6.87
EMSC-2016-0130_a	0.41	27.35	4.81

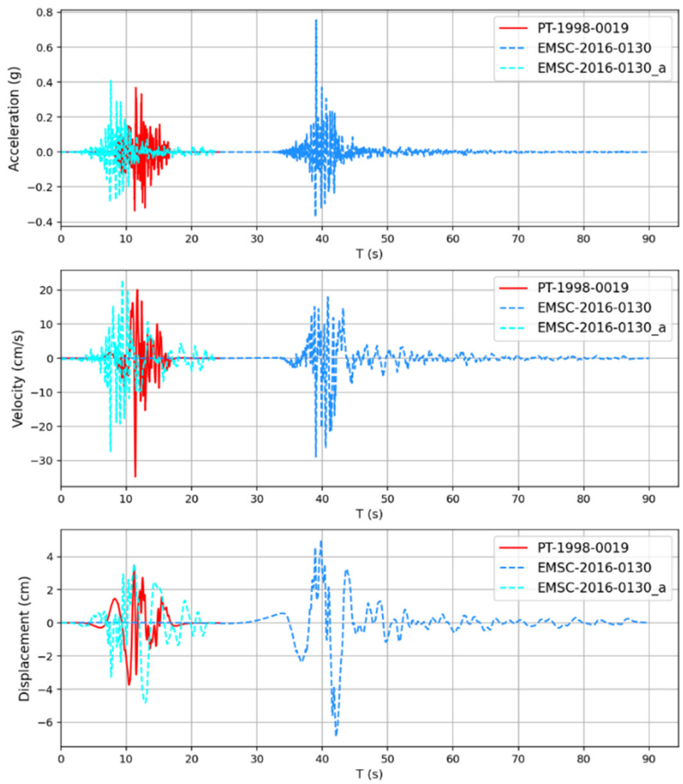

Fig. 7: Time histories of the acceleration, velocity and displacement of the selected signals

The testing program was based on an Incremental Dynamic Testing (IDT) run using PT-1998-0019, with a 25% increment in signal amplitude, while EMSC-2016-0130_a was applied only twice at a high scale factor (SF) in its original and reversed directions, to investigate the directivity effects in the original record. Before testing, each SF was tuned on the shake table against the simulated mass of the specimen. Such a step is essential to accurately reproduce the desired input without prematurely damaging the specimen.

Acquisition and validation

A DIC system with six medium-to-high-speed cameras installed along the perimeter of the shake table enabled data acquisition and extraction of the displacements. The displacements were extracted from the points recorded on the speckle patterns glued on all the blocks. Before conducting the campaign, the validation of the setup boundary conditions was required. The validation was done by comparing the OOP displacements of the left-centred block in the first course of the façade (see Acc 10 in **Error! Reference source not found.**) concerning the injected signal. While Fig. 8a shows the validation for the test with 100% SF, Fig. 8b shows the validation for the test with 160% SF.

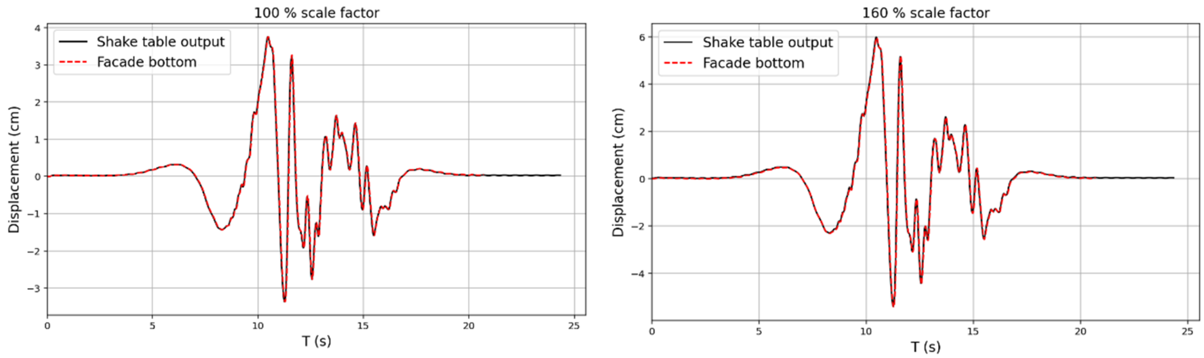

a) b)

Fig. 8: Validation of the bottom boundary condition: a) SF 100%, b) SF 160%

From Fig. 8, it is possible to observe that the total restraint of the bottom boundary condition was achieved. The next Section presents the test results and the observed failure mechanisms on the U-shape specimen.

DISCUSSION OF THE TEST RESULTS

The summary of the tests is listed in Table 3. The acronym of each test identifies the tested specimen (US), the vertical slenderness (λ=9), the height-to-length façade ratio (H/B =1.25), the acronym of the station where the seismic event was recorded (HOR/EMSC), and the SF (025, …). For each test, Table 3 reports the values of the Peak Ground Acceleration (PGA), the Peak Ground Velocity (PGV), and the maximum OOP displacements recorded at four points in the façade. These points were chosen from Fig. 5 as follows: a) Acc 7 = Point 1 (P1), Acc 1 = Point 2 (P2), Acc 2 = Point 3 (P3), and Acc 4 = Point 4 (P4).

At low intensities of PT-1998-0019 (up to 100% SF), the corners were observed rotating around the vertical hinge and displacing in the OOP direction. This response was confirmed by the presence of a vertical crack stepping through the intersection between the return walls and the façade. Also, OOP displacements were observed in the return walls, with IP diagonal cracks stepping from the top side of the return wall to several height levels in the façade. This pattern suggested the initiation of façade rocking that included portions of the return walls. Also, this behavior was observed to be in line with the first mode shape extracted during the dynamic acquisition tests. By increasing the signal amplitude, such a response became more pronounced. At a PTA of 0.496 g and a PTV of 33.72 cm/sec (120% SF), the return walls underwent large deformation in the OOP direction. Furthermore, at a PTA of 0.62 g and PTV of 42.123 cm/s, the specimen exhibited collapse showing the targeted hybrid mechanism. Overall, as reported in Table 3, the specimen responded asymmetrically between the corners, however, the latter equally participated in all the collapses. The IDT sequence was terminated when the specimen exhibited three collapses in sequence. Fig. 10 shows the U-shape response at increasing SFs in the facade, while Fig. 10 on the return walls.

Table 3: Summary of the dynamic tests on the U-Shape

Test ID	PGA (g)	PGV (cm/s)	Maximum OOP displacement				Test result
			P1 (cm)	P2 (cm)	P3 (cm)	P4 (cm)	
US_9_1.25_HOR_025	0.104	7.004	0.018	0.0107	0.101	0.076	No collapse
US _9_1.25_HOR_050	0.214	13.846	0.073	0.171	1.050	0.494	No collapse
US _9_1.25_HOR_060	0.253	16.784	0.244	0.848	1.013	0.195	No collapse
US _9_1.25_HOR_075	0.293	21.006	0.523	0.956	2.854	1.311	No collapse
US _9_1.25_HOR_080	0.313	22.757	0.714	2.243	2.432	0.918	No collapse
US _9_1.25_HOR_090	0.346	25.820	0.92	2.749	3.147	1.494	No collapse
US _9_1.25_HOR_100	0,391	27.997	1.253	3.686	7.323	4.556	No collapse
US _9_1.25_HOR_110	0.432	30.745	1.709	5.366	6.555	3.386	No collapse
US _9_1.25_HOR_115	0.460	32.159	2.118	6.797	8.577	4.136	No collapse
US _9_1.25_HOR_120	0.496	33.720	2.652	6.056	10.091	5.443	No collapse
US _9_1.25_HOR_130	0.525	36.522	3.460	8.094	12.588	7.654	No collapse
US _9_1.25_HOR_140	0.563	39.401	4.042	9.489	15.405	12.053	No collapse
US _9_1.25_HOR_150	0.620	42.123	4.89	*	*	*	Collapse
US _9_1.25_HOR_160	0.654	44.974	5.474	12.876	20.149	17.751	No collapse
US _9_1.25_HOR_170	0.701	47.511	7.142	*	*	*	Collapse
US _9_1.25_HOR_175	0.745	49.424	8.706	18.792	24.208	19.997	No collapse
US _9_1.25_HOR_180	0.752	50.735	9.161	*	*	*	Collapse
US _9_1.25_HOR_190	0.766	52.656	9.977	*	*	*	Collapse
US _9_1.25_HOR_200	0.812	54.292	7.912	*	*	*	Collapse
US _9_1.25_MZ28_026_240	0.959	65.018	7.422	9.569	*	9.131	Collapse
US _9_1.25_MZ28_026_240_rev	0.917	64.092	6.17	8.95	*	*	Collapse

* Indicates the collapse occurrence

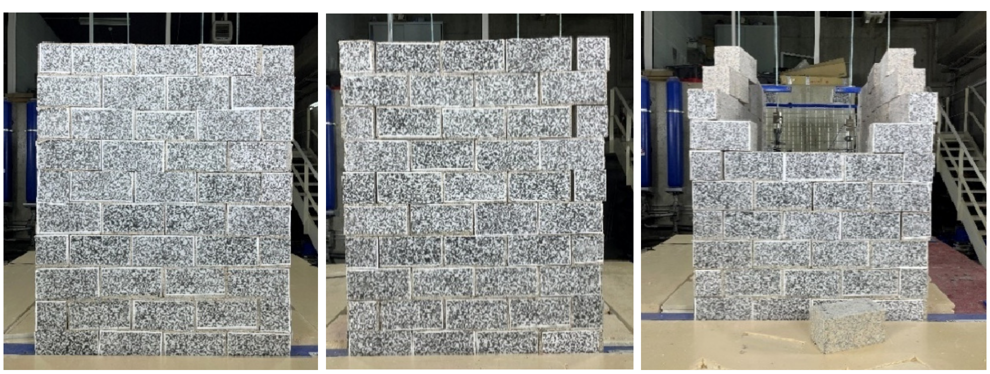

a) b) c)

Fig. 9: Main façade response during the IDT run: a) 50% SF, b) 120% SF, c) 150% SF

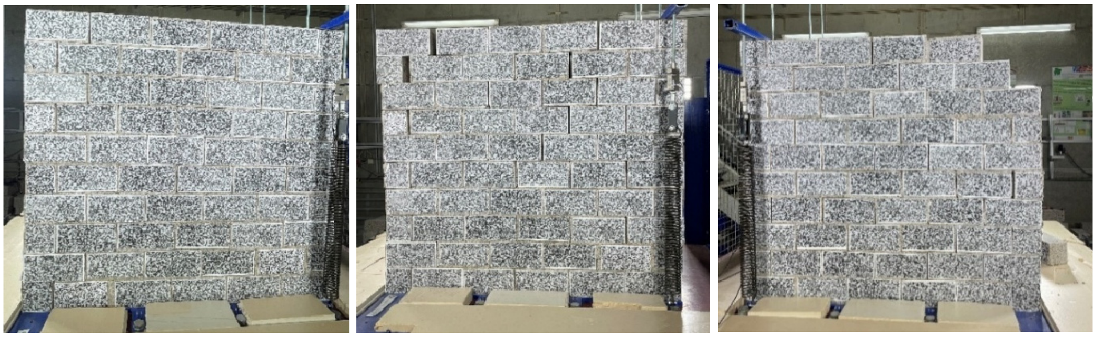

a) b) c)

Fig. 10: Return walls response during the IDT run: a) 50% SF (east return wall), b) 120% SF (east return wall), c) 150% SF (west return wall)

Under the application of EMSC-2016-0130_a, the specimen showed a different response. Despite being filtered, the high-frequency content in the acceleration time history seemingly led to a more complex failure mechanism. The two top corner blocks did not experience collapse, unlike the central blocks, showing a more pronounced vertical rather than horizontal bending. The return walls showed large shear cracking; however, the overturning of the façade did not occur, hence the targeted mechanism was not achieved. **Error! Reference source not found.** a) shows the response of the U-shape under EMSC-2016-0130_a in the main façade, while **Error! Reference source not found.** b) on the east return wall.

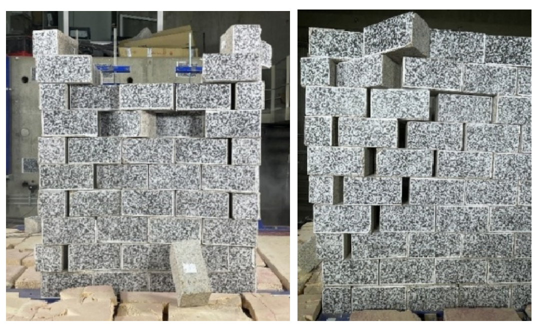

a) b)

Fig. 11: U-shape collapse under EMSC-2016-0130_a: a) main façade, b) east return wall

The response under the reversed EMSC-2016-0130_a indicated the presence of directivity effects in the original signal. At the collapse occurrence, the façade exhibited an inward rather than outward collapse. The reversed EMSC-2016-0130_a again led to vertical bending of the upper half of the façade. The acceleration content was able to trigger a pronounced IP deformation; however, the velocity content was not enough for the overturning, hence the hybrid mechanism was not achieved. Fig. 12 a) shows the collapse mechanism in the façade, while Fig. 12 b) shows the collapse of the main façade together with the west return wall.

a) b)

Fig. 12: U-shape collapse under the reversed EMSC-2016-0130_a: a) main facade, b) main façade and west return wall.

Despite the same boundary conditions, these findings showed that signals with different characteristics could induce different OOP collapse mechanisms. Overall, the self-weight of the structure played a role in the response. Considering the block's weight (18kg each), when subjected to the first input, only two top courses of the U-Shape participated in the failure, while most of the structure underwent rocking without large out-of-plane displacement. The leading horizontal hinge around which the overturning occurred was observed to be at the second course from the top. According to the literature, this hinge can form between 0.55 and 0.75 H (height) of a structure when considering a 2D problem such as a vertically spanning strip wall. By increasing the load (or precompression state) the hinge can shift upwards. Differently, the final horizontal hinge in the U-Shape was observed around 0.8 H of the structure, despite the absence of any precompression load applied on the facade. The upwards shift may be attributed to self-weight. In addition, the self-weight contribution was observed when the specimen was subjected to the second input, with higher inertia forces in each block due to the acceleration content.

CONCLUSIONS

This contribution has presented a shake table campaign carried out at the Structures Laboratory of the University of Minho. The campaign was designed to accommodate a very large number of tests on a dry-stack half-scale specimen made of a façade and two return walls (U-Shape). The tests were planned to target a complex hybrid mechanism including diagonal-shear cracking in the return wall, bending and failure due to overturning in the façade. The tests have shown that different recorded ground motions (pulse-like and non-pulse-like) lead to substantial changes in the response. While the former led to failure due to facade overturning, hence to the targeted hybrid mechanism, the latter induced high vibration in each block, leading to disintegration failure. The present campaign is currently ongoing, and it is including a second geometry subjected to the same recorded ground motions. Data generated are essential to calibrate models and to obtain experimentally based fragility curves to be compared with numerical ones. Upon validation of modelling strategies, upscaling of the models to real size will be possible and validation of current code-based safety assessment procedures may be further enhanced.

ACKNOWLEDGEMENTS

This investigation has been partly funded by the STAND4HERITAGE project that has received funding from the European Research Council (ERC) under the European Union's Horizon 2020 research and innovation program (Grant agreement No. 833123), as an Advanced Grant. This work was also partly financed by FCT/MCTES through national funds (PIDDAC) under the R&D Unit Institute for

Sustainability and Innovation in Structural Engineering (ISISE), under reference UIDB/04029/2020, and under the Associate Laboratory Advanced Production and Intelligent Systems ARISE under reference LA/P/0112/2020.

REFERENCES

[1] TEBC, "Turkish building earthquake code," T.C. Resmi Gazete, Ankara, Turkey, 2019.

[2] G. Ozkula *et al.*, "Field reconnaissance and observations from the February 6, 2023, Turkey earthquake sequence," *Natural Hazards*, vol. 119, no. 1, pp. 663–700, 2023, doi: 10.1007/s11069-023-06143-2.

[3] D. Dizhur *et al.*, "Performance of masonry buildings and churches in the 22 February 2011 Christchurch earthquake," *Bulletin of the New Zealand Society for Earthquake Engineering*, vol. 44, no. 4, pp. 279–296, 2011, doi: 10.5459/bnzsee.44.4.279-296.

[4] A. Penna *et al.*, "Damage to churches in the 2016 central Italy earthquakes," *Bulletin of Earthquake Engineering*, vol. 17, no. 10, pp. 5763–5790, 2019, doi: 10.1007/s10518-019-00594-4.

[5] G. De Felice and R. Giannini, "Out-of-plane seismic resistance of masonry walls," *Journal of Earthquake Engineering*, vol. 5, no. 2, pp. 253–271, 2001, doi: 10.1080/13632460109350394.

[6] D. D'Ayala and E. Speranza, "Definition of Collapse Mechanisms and Seismic Vulnerability of Historic Masonry Buildings," *Earthquake Spectra*, vol. 19, no. 3, pp. 479–509, 2003, doi: 10.1193/1.1599896.

[7] L. Sorrentino, R. Masiani, and M. C. Griffith, "The vertical spanning strip wall as a coupled rocking rigid body assembly," *Structural Engineering and Mechanics*, vol. 29, no. 4, pp. 433–453, Jul. 2008, doi: 10.12989/sem.2008.29.4.433.

[8] K. Doherty, M. C. Griffith, N. Lam, and J. Wilson, "Displacement-based seismic analysis for out-of-plane bending of unreinforced masonry walls," *Earthq Eng Struct Dyn*, vol. 31, no. 4, pp. 833–850, 2002, doi: 10.1002/eqe.126.

[9] G. W. Housner, "The behavior of inverted pendulum structures during earthquakes," *Bulletin of the Seismological Society of America*, vol. 53, no. 2, pp. 403–417, 1963, doi: 10.1785/bssa0530020403.

[10] P. B. Lourenço, J. M. Leite, M. F. Paulo-Pereira, A. Campos-Costa, P. X. Candeias, and N. Mendes, "Shaking table testing for masonry infill walls: unreinforced versus reinforced solutions," *Earthq Eng Struct Dyn*, vol. 45, no. 14, pp. 2241–2260, Nov. 2016, doi: 10.1002/eqe.2756.

[11] N. Mendes, P. B. Lourenço, and A. Campos-Costa, "Shaking table testing of an existing masonry building: Assessment and improvement of the seismic performance," *Earthq Eng Struct Dyn*, vol. 43, no. 2, pp. 247–266, 2014, doi: 10.1002/eqe.2342.

[12] P. B. Lourenço, L. Avila, G. Vasconcelos, J. P. P. Alves, N. Mendes, and A. C. Costa, "Experimental investigation on the seismic performance of masonry buildings using shaking table testing," *Bulletin of Earthquake Engineering*, vol. 11, no. 4, pp. 1157–1190, Aug. 2013, doi: 10.1007/s10518-012-9410-7.

[13] J. Vaculik, M. C. Griffith, and G. Magenes, "Dry stone masonry walls in bending-Part II: Analysis," *International Journal of Architectural Heritage*, vol. 8, no. 1, pp. 29–48, 2014, doi: 10.1080/15583058.2012.663060.

[14] F. Graziotti, U. Tomassetti, S. Sharma, L. Grottoli, and G. Magenes, "Experimental response of URM single leaf and cavity walls in out-of-plane two-way bending generated by seismic excitation," *Constr Build Mater*, vol. 195, pp. 650–670, Jan. 2019, doi: 10.1016/j.conbuildmat.2018.10.076.

[15] J. Vaculik and M. C. Griffith, "Out-of-plane shaketable testing of unreinforced masonry walls in two-way bending," *Bulletin of Earthquake Engineering*, vol. 16, no. 7, pp. 2839–2876, Jul. 2018, doi: 10.1007/s10518-017-0282-8.

[16] P. Morandi *et al.*, "Dynamic shaking table out-of-plane tests on weak masonry infills with and without previous in-plane loading," *Journal of Building Engineering*, p. 111670, 2024, doi: 10.1016/j.jobe.2024.111670.

[17] G. Vlachakis, C. Colombo, A. I. Giouvanidis, N. Savalle, and P. B. Lourenço, “Experimental characterisation of dry-joint masonry structures: Interface stiffness and interface damping,” *Constr Build Mater*, vol. 392, Aug. 2023, doi: 10.1016/j.conbuildmat.2023.130880.
[18] A. C. Costa, A. Arêde, A. Campos Costa, A. Penna, and A. Costa, “Out-of-plane behaviour of a full scale stone masonry façade. Part 1: specimen and ground motion selection,” *Earthq Eng Struct Dyn*, no. 42, pp. 2081–2095, 2013, doi: 10.1002/eqe.
[19] A. C. Costa, A. Arêde, A. Campos Costa, A. Penna, and A. Costa, “Out-of-plane behaviour of a full scale stone masonry façade. Part 2: shaking table tests,” *Earthq Eng Struct Dyn*, no. 42, pp. 2097–2111, 2013, doi: 10.1002/eqe.
[20] D. S. Panella, M. E. Tornello, and C. D. Frau, “A simple and intuitive procedure to identify pulse-like ground motions,” Mar. 01, 2017, *Elsevier Ltd*. doi: 10.1016/j.soildyn.2017.01.020.